Article:
Liu, C, Chen, X orcid.org/0000-0002-2053-2448, Mack, EE et al. (5 more authors) (2019) Evaluating a novel permeable reactive bio-barrier to remediate PAH-contaminated groundwater. Journal of Hazardous Materials, 368. pp. 444-451. ISSN 0304-3894

https://doi.org/10.1016/j.jhazmat.2019.01.069

Evaluating a novel permeable reactive bio-barrier to remediate PAH-contaminated groundwater

Cuicui Liu[a], Xiaohui Chen[b], E. Erin Mack[c], Shui Wang[d], Wenchao Du[e], Ying Yin[a], Steven A. Banwart[f,g], Hongyan Guo[a,*]

[a]State Key Laboratory of Pollution Control and Resource Reuse, School of the Environment, Nanjing University, Nanjing 210023, China

[b]School of Civil Engineering, University of Leeds, Leeds LS2 9JT, UK

[c]DuPont Corporate Remediation Group, Wilmington, DE 19805, USA

[d]Jiangsu Provincial Academy of Environmental Science, Nanjing 210036, China

[e]School of the Environment, Nanjing Normal University, Nanjing 210023, China

[f]School of Earth and Environment, University of Leeds, Leeds LS2 9JT, UK

[g] Global Food and Environment Institute, University of Leeds, Leeds, LS2 9JT, UK

*Correspondence: Hongyan Guo, tel.: +8613813945566, fax: +86-25-89680263.

E-mail: hyguo@nju.edu.cn

Abstract

Permeable reactive barriers (PRBs) are an environmentally-friendly, cost-effective *in-situ* technology that can be used to remediate polycyclic aromatic hydrocarbons (PAHs)-contaminated groundwater. In this study, PRB of two various materials (A and B) that relied on microbes self-domestication mechanism were designed and tested. The materials A and B were the same apart from their carbon source: A was based on wheat straw and B was based on coconut shell biochar. We used laboratory batch experiments followed by long-term column tests to assess the capacity of these two materials to remediate PAHs. The results showed that both A and B removed almost 100% of the phenanthrene. More carbon was released from A (80–500 mg/L) than from B (72–195 mg/L), and slightly more oxygen was released from B (7.31–10.31 mg/L) than A (7.15–9.64 mg/L). The release of organic carbon from material B was more stable than that from material A. The bacterial communities of both columns comprised members of the Mycobacterium, Pseudomonas, and Sphingomonas genera that are known to degrade phenanthrene, and Pseudomonas and Sphingomonas were 7 times more abundant in column B than in column A. Material B is more promising for treating PAH-contaminated groundwater than material A.

Keywords: Microbe; Self-domestication; Phenanthrene; Groundwater remediation; Permeable reactive biobarrier

1. Introduction

Polycyclic aromatic hydrocarbons (PAHs) present serious environmental risks and are common in various environmental media [1,2]. Even at low concentrations, PAHs can be toxic to various organisms and are potentially mutagenic and carcinogenic to humans [3,4]. In China, studies have reported that groundwater from 69 cities in 31 provinces was severely polluted by organic contaminants [5], and that the groundwater in Northern, Northeastern, Southeastern, and Southwestern China was severely polluted by PAHs [6-10]. Research has shown that PAHs can be biodegraded to CO_2 and H_2O by microbial communities under aerobic conditions [11,12], and that the rate of biodegradation depends on the pH, oxygen levels, microbial population, and the accessibility of nutrients [12]. Lee et al. [13] suggested that the microbial growth, and therefore the rate of PAH degradation, could be stimulated and enhanced by adding carbon in the form of pyruvate. The dissolved oxygen (DO) content in groundwater is usually very low (below 3 mg/L) [14]. The biodegradation of PAHs may be limited by the low oxygen levels in the groundwater and by constraints on mass-transfer caused by the relatively low solubility of PAHs. The main challenges, therefore, for *in situ* bioremediation of PAHs are the choice of a suitable carbon substrate and the oxygen supply.

Calcium peroxide and straw/biochar have potential to be used in PRBs but, to date, they have infrequently been used in PAHs biodegradation applications. Huang et al. [15] reported that an oxygen-releasing compound (ORC) that included calcium and

magnesium peroxide could efficiently supply sufficient oxygen to sustain approximately 120 pore volumes. Lin et al. [16] found that encapsulated oxygen-releasing beads consistently released oxygen over 128 days when bioremediating groundwater contaminated by BTEX at high concentrations. Biochar is a carbonaceous porous material that is economical and readily available [17]. Other low-cost materials that have already been considered as carbon sources for groundwater remediation in previous studies include human and livestock waste [18]; cotton [19]; wheat straw, sawdust, and biodegradable plastics [20]; maize stalks [21]; cassava distiller's dried grains [22]; biodegradable snack ware [23], and paper [24]. Other studies have used materials such as liquor [25], biodegradable polymers [26], polybutylene succinate or polylactic acid-based composites [27], rice washing drainage water [28], and soluble starch [29] as carbon sources when remediating groundwater. However, these products are less suitable for PRB applications as they are costly and are mobile and may be washed out of a barrier.

Permeable reactive barriers (PRBs) provide a mature remediation technology that has been used to treat groundwater for decades [30-35]. Studies have shown that PRBs can successfully remove a wide variety of contaminants, including heavy metals, chlorinated solvents, aromatic hydrocarbons, and pesticides [36]. The removal efficiency of the PRB depends on the type of reactive media used and the removal mechanism. Different PRB media have been studied to determine their ability to remove inorganic contaminants such as metals, nitrates, and organic contaminants,

particularly chlorinated solvents [37, 38]. However, PRBs have not been widely used to remove PAHs, perhaps because the available reactive media are limited [39].

Various reactive materials have already been used to remediate PAH-contaminated groundwater including zero-valent iron, zeolite, and activated carbon mixtures [40]; organoclays [41]; zeolites [42]; flyash [43]; Trichoderma longibrachiatum [44]; Arthrobacter viscosus [1]; Pseudomonas stutzeri CECT 930 [45], and microbes along with granular activated carbon [46]. In groundwater, PAHs are mainly degraded by microbes [47], and PAHs with less than five rings are usually biodegraded by bacteria under aerobic conditions [48]. *In situ* bioremediation includes biostimulation and bioaugmentation. During biostimulation, the activity of the intrinsic microorganisms is stimulated to biodegrade the organic contaminants by adding oxygen and injecting a large quantity of inorganic nutrients or suitable electron donors/acceptors into the groundwater. This method is slow and, to date, has not been very effective [50]. In bioaugmentation, microorganisms with biodegradation ability are injected and oxygen and inorganic nutrients are added to accelerate the biodegradation of pollutants [49]. This method is challenged by the need to sustain the catabolic activity of the bacteria at low pollutant concentrations [51]. Also, it is not cost-effective to cultivate the specialized bacterial strains with specific metabolic capabilities that are needed to degrade the pollutants [52].

The objective of the present study was to evaluate an application of new reactive materials in PRBs that used a microbe self-domestication mechanism to remediate

phenanthrene-contaminated groundwater. The suitability of the materials was evaluated from (i) the extent of phenanthrene biodegradation, (ii) the duration of carbon and oxygen release, and (iii) the change in the relative abundance of biodegradable bacteria. These objectives were investigated using batch experiments and long-term column experiments. The batch experiments provided information about the removal efficiency of phenanthrene by the reactive materials, and the column experiments provided information about the extent of phenanthrene biodegradation, the longevity of the reactive materials, and the growth of biodegradable bacteria.

2. Materials and methods

2.1. Preparation of PRB materials

The PRB slow-release materials A and B were both three-dimensional pellets that had a three-layer structure, a core, a packed layer, and an outer shell. Both materials had a wood brick core, but the packed layer in material A was composed of wheat straw mixed with diatomite, attapulgite, and calcium peroxide, while that in material B was composed of coconut shell biochar, also mixed with diatomite, attapulgite, and calcium peroxide. The outer shell of materials A and B was made of attapulgite, diatomite, and Portland cement. The only difference between materials A and B was the carbon source in the packed layer. The materials were bound by sodium alginate mixed with water. All the raw materials in this study were used without further purification. The basic characteristics of the components are shown in Table S1.

2.2. Brunauer-Emmett-Teller (BET) surface area

The Brunauer-Emmett-Teller (BET) surface area and porosity of materials A and B at the beginning were characterized using a specific surface area and porosity analyzer (ASAP 2020, Micromeritics Instrument Corp., USA) after degassing for 8 h at 70 and 100 °C, respectively.

2.3. Batch adsorption and static experiments

Materials A and B (1 g of each) were added to 250 mL glass flasks with glass lids. Each material was mixed with 150 mL of 0.9 mg/L phenanthrene solution with sodium azide (200 mg/L) to eliminate any possible microbial degradation by native microorganisms. All experiments were conducted in triplicate. The flasks were shaken (200 rpm) for 510 min at 25 °C to ensure that the adsorption reached equilibrium.

A fixed amount (2 g) of materials A and B were added to 100 mL of phenanthrene solution (0.9 mg/L in deionized water) in a 100 mL sealed conical flask and thoroughly mixed in the dark. After 5 days, samples were collected from the flasks and analyzed for DO (data shown in Figure S1) and phenanthrene. Meanwhile, the solution in the flask was replaced with an additional 100 mL of the phenanthrene solution. This process was repeated fourteen times.

2.4. Column experiments

We analyzed the results of the batch experiments, and then set up a continuous flow column experiment to determine the ability of materials A and B to remove phenanthrene. The glass columns were 50 cm long, with an inner diameter of 4 cm, and a volume of 628 mL. They were equipped with sampling ports at the influent, effluent, and 4 sampling ports (named 1–4), each with a diameter of 0.5 cm and spaced at 10 cm intervals along the column. The columns were packed with a homogenous mixture of either material A or B and quartz sand (1:1, v/v). The materials in the columns were bounded by 5 cm-layers of sand at both the bottom and the top. Column A contained 663.5 g of quartz sand and 250.5 g of material A and had a porosity of 23.6% and a pore volume of 148.2 mL. Column B contained 677 g of quartz sand and 238.5 g of material B and had a porosity of 24.1% and a pore volume of 151.3 mL. The configuration of a treatment column is illustrated in Fig. 1.

We used an unsterilized solution of deionized water and 0.9 mg/L phenanthrene for the contaminated groundwater. The solution was pumped upwards through the columns at a constant flow rate of 126.89 $\mu L \cdot min^{-1}$ and a retention time of 24.93 h. The flow was uniform over the 450-day experimental period. The system was operated in dark oxic conditions.

The pH, DO, TOC, and phenanthrene concentrations of the effluent samples were determined. The pH and DO were measured immediately after samples were collected using a portable analyzer (Orion 5 Star, Thermo, USA). The TOC concentrations were determined using a total organic carbon analysis meter (TOC-Aurora 1030D, OI, US).

Part of the sample was centrifuged at 10000 rpm for 15 min, and then the phenanthrene concentrations were determined on the supernatant using high performance liquid chromatography (HPLC 1200, Agilent, USA) equipped with a reverse phase column (Supelco Discovery C-18) that was 25 cm long, with a diameter of 4.6 mm, and an internal diameter of 5 μm. The injection volume was set at 30 μL, and the isocratic eluent (90:10 methanol/water) was pumped at a rate of 1 mL/min for 6.5 min. The UV wavelength was set at 254 nm, and the column temperature was maintained at 30 °C. The limit of detection (LOD) of the method for the target phenanthrene was 0.01 mg/L.

2.5. Environmental Scanning Electron Microscopy (ESEM)

After the column experiment had run for 200 days, samples of materials A and B were collected and fixed with 2.5% glutaraldehyde in a 0.1 M phosphate buffer (pH 7.3) at 4 °C for 12 h, washed 3 times in a 0.1 M phosphate buffer at 4 °C (pH 7.3) for 10 min, and then dehydrated in an ethanol/water mixture (50%, 70%, 80%, 90%, 95%, and 100%) for 10 min. After this, the samples were treated with hexamethyldisilazane (HMDS) by immersing them twice for 30 s in pure HMDS and then were air-dried for 10 min [53]. Finally, the dried samples were sputter-coated with gold with an auto-sputter coater (AGAR, Germany) and the surface topography was analyzed using environmental scanning electron microscopy (ESEM, FEI Quanta 250 FEG, USA) at an accelerating voltage of 10 kV with a working distance of 10 mm.

2.6. Analysis of the microbial communities

Samples of materials A and B at the beginning of the experiment were sealed and stored at −80°C to inhibit the growth of microorganisms. After the column experiment had run for 200 days, samples of the materials were collected from the sampling ports in columns A and B and were placed in plastic 50 mL tubes and stored at −20 °C to minimize bacterial growth [54]. Subsamples (0.5 g) were taken from these samples and the DNA were extracted using a FastDNA^{TM} SPIN Kit for soil.

The V4 region of the bacterial 16S rRNA gene was amplified using the 515F (5'-GTGCCAGCMGCCGCGGTAA-3') and 806R (5'-GGACTACHVGGGTWTCTAAT-3') primers for pyrosequencing on a sequencer (MiSeq) [55,56]. The PCR amplification reaction mixture (25 μL) contained 1×PCR buffer, 1.5 mM $MgCl_2$, 0.4 μM deoxynucleoside triphosphate, 1.0 μM primer, 0.5 U of Ex Taq (TaKaRa, Dalian), and 10 ng of the genomic DNA extracted from materials A and B. The PCR amplification program included initial denaturation at 94 °C for 3 min, followed by 30 cycles of 94 °C for 40 s, 56 °C for 60 s, 72 °C for 60 s, and a final extension at 72 °C for 10 min. The PCR products were examined using 1.0% agarose gel. The band was excised and purified using a San Prep DNA Gel Extraction Kit (Sangon Biotech, China，Cat# SK8132) and quantified with Nanodrop. The sequencing samples were prepared using a TruSeq DNA kit according to the manufacturer's instructions. The purified amplicons were pooled in equimolar and sequenced on an sequencing platform (Illumina Miseq), according to the standard protocols. The raw reads were deposited in the NCBI

Sequence Read Archive (SRA) database under accession number SRS1829960.

The raw sequences were processed using the QIIME pipeline, Version 1.7.0 (http://qiime.org/). All the sequence reads were trimmed and assigned to each sample based on their barcodes. The sequences with high quality (defined as having a length > 150 bp, without ambiguous base Ns, and an average base quality score > 30) were used for downstream analysis. Sequences were clustered into operational taxonomic units (OTUs) based on an identity threshold of 97%. All the samples were randomly resampled to 10638 reads. The taxonomy was assigned using the Ribosomal Database Project Classifier [57].

2.7. Desorption experiments

After the column experiment had run for 450 days, we tested the desorption from samples of materials A and B collected from the sampling ports in columns A and B. The material (0.5 g) and 10 mL of 100 mg/L surfactant solution that contained 200 mg/L of NaN_3 as a bio-inhibitor were added to 40 mL glass tubes. The tubes were shaken at 20 °C and 200 rpm for 24 h to reach the desorption equilibrium [58].

3. Results and discussion

3.1. BET surface area

The specific surface areas of materials A and B were determined with the classic BET method (Fig. 2). The BET surface area, pore volume, and pore size of A were 8.62 m^2

g^{-1}, 0.02 $cm^3\ g^{-1}$, and 6.33 nm, respectively. The BET surface area, pore volume, and pore size of B were 89.33 $m^2\ g^{-1}$, 0.05 $cm^3\ g^{-1}$, and 3.79 nm, respectively. The BET surface area of B was 10 times that of A, possibly resulting in its stronger capacity to adsorb phenanthrene.

3.2. Adsorption and static experiments

The adsorption equilibrium time is an important control parameter for pollutant remediation, which in turn affects the practicality and design parameters of PRBs [59]. The adsorption kinetics of phenanthrene for materials A and B are presented in Fig. 3. The maximum phenanthrene adsorption capacities of materials A and B were determined as 0.013 and 0.035 mg/g, respectively, from the batch experiment data. With only 9.6% removal at 510 min, the kinetics and phenanthrene removal capacity of material A were low. In contrast, the uptake of material B was more rapid, and removal of 26.1% was achieved at 510 min with 23.7% of the adsorption capacity filled in the first 300 min. These results indicate that material B has a better adsorption capacity than material A.

The phenanthrene removal efficiency by materials A and B is shown in Fig. 4. Material A removed between 8% and 72% (a total of 0.35 mg), and B removed between 8% and 100% (a total of 0.55 mg), of the first 10 doses of phenanthrene. Material B showed a stronger affinity for phenanthrene in deionized water than A, and removed almost 100% of the phenanthrene in the ninth dose. But, in later doses, A and B both

showed high removal efficiencies (> 97%). These data indicate that both materials were capable of removing phenanthrene.

3.3. Column experiments

In the column experiments, a PRB system was simulated and the removal rate of phenanthrene was evaluated. The temporal variation in the pH, DO, and TOC concentrations in the influent and effluent are shown in Figs. 5a–c.

pH analysis: The changes of the pH in samples collected from sampling ports (SP1, SP2, SP3, and SP4) in columns A and B after 200 days are presented in Fig. 5a. The pH gradually increased in columns A and B, perhaps because $Ca(OH)_2$ formed from the oxygen source, CaO_2, and caused the pH to rise. The Portland cement may also have contributed to the increase in the pH.

DO: The variations in the DO in the influent and effluent over the operational period are presented in Fig. 5b. The DO in the influent ranged from 5.57 to 6.01 mg/L. The DO concentrations in the effluent of columns A and B were higher than those in the influent between days 3 and 350, and the DO concentrations increased clearly from days 3 to 200. Later in the experiment, the DO concentrations in the effluents from A and B were slightly higher than those in the influent. These data indicate that the CaO_2 incorporated in materials A and B acted as a slow-release source of oxygen and possibly also supported the aerobic microbes that degraded the phenanthrene over 350 days, which is considered as a reasonably long time.

TOC: The changes in the TOC concentrations in the influent and effluent of the columns during the operation period are shown in Fig. 5c. The TOC concentration in the influent was relatively stable and ranged from 142 to 167 mg/L. The TOC concentration in the effluent from column A reached 500 mg/L during the first 3 days, but then decreased and was between 80 and 160 mg/L in the remaining days. In contrast, the TOC concentration in the effluent from column B remained relatively stable and ranged from 72 to 195 mg/L. The organic carbon is known to affect the structures of microbial communities, and it can be a carbon source for microorganisms [60]. Indeed, high rates of microbial respiration are partly caused by the high concentrations of dissolved organic matter. Hence, an increase in the availability of organic carbon could enhance the rates of microbial respiration [61]. When the concentration of phenanthrene is low or inconsistent over time because of its low solubility [62], organic carbon may help to maintain a population of phenanthrene-degrading organisms. Lee et al. [13] suggested that carbon stimulated microbial growth and enhanced the rate of PAH degradation. Hence, when released, organic carbon could enhance the rate of phenanthrene degradation in certain conditions.

The removal efficiency of phenanthrene was close to 100% in columns A and B during the whole operation phase, which shows that materials A and B could effectively remove phenanthrene from groundwater. These removal efficiencies are higher than those reported in previous studies. Cobas et al. [44] used Trichoderma longibrachiatum as PRB media and achieved 90% removal. Zhou et al. [40] achieved 94.2% removal

with a combination of zero-valent iron, zeolite, and activated carbon. The results from this study show that materials A and B could be used to removing PAHs from groundwater in PRBs.

3.4. Surface morphology by ESEM

The ESEM images show how the surface morphology of A and B changed over the course of the experiment (Fig. 6). Initially, A had a smooth surface (Fig. 6A), while B had a more roughly-structured surface (Fig. 6B). After 200 days, the surfaces of A and B were mushroom-like and their microstructures were very different from how they were at the beginning (Figs. 6C–D).

3.5. Changes in the structures of the microbial communities in the columns

The results from principle coordinated analysis (PCoA) using weighted UniFrac metrics showed that bacterial community present in the 16S rRNA genes of the column A was very different from that in column B (Fig. 7a). The first axis explained 59.83% of the variation. Samples from both columns were well separated along this axis, which indicates that the bacterial communities of columns A and B were very different.

The change in overall population, i.e., the difference between the total numbers of eubacterial 16S rDNA genes in the initial material and in samples collected during the experiment, are presented in Fig. 7b. The 16S rDNA genes in samples from ports SP1, SP2, and SP3 were higher than those in the initial material in columns A and B. If we

compared the relative abundances of the bacterial taxa in columns A and B, we could find out which organisms controlled the processes in the PRB [63]. Bacterial degradation of phenanthrene has been studied with different genera of *Mycobacterium*, *Pseudomonas*, and *Sphingomonas* [11,64,65]. As shown in Fig. 7c, the relative abundance of phenanthrene-degradation bacteria, from the genus *Mycobacterium*, *Pseudomonas*, and *Sphingomonas*, increased over the course of the experiment, which indicates that these genera were positively correlated with the high removal efficiency of phenanthrene. The fact that the abundance of phenanthrene-degrading genera was higher in column B than in column A may be due to the differences between the materials in the columns.

3.6. Phenanthrene desorption of materials A and B

The desorption concentrations of phenanthrene in solid samples from the sampling ports of columns A and B are shown in Table 1. The desorption concentration of phenanthrene was low and the maximum phenanthrene adsorption capacities of materials A and B were 0.013 and 0.035 mg/g, respectively. Columns A and B contained 250.5 and 238.5 g of material, respectively. Therefore, maximum amounts of 3.26 and 8.35 mg of phenanthrene were adsorbed by columns A and B, respectively. A total of 58.3 mg of phenanthrene passed through the column over the 450 days of operation, which suggests that there was significant degradation of phenanthrene within the column. These data indicate that the materials combined adsorption and degradation

mechanisms to remove phenanthrene.

3.7. Analysis of the longevity of the slow-release materials

The shell of the slow-release materials used in this study was manufactured using attapulgite, diatomite, and Portland cement. Attapulgite is a type of hydrated octahedral layered magnesium aluminum silicate absorbent mineral with exchangeable cations and reactive −OH groups on its surface [66]. Diatomite ($SiO_2 \cdot nH_2O$) is a fine granulated siliceous sedimentary rock, mainly composed of diatom shells with smaller proportions of other sediments like clay and quartz [67]. Portland cement is made of clay and limestone, which is mostly calcium oxide, silica, and alumina [68]. Silicate, which is naturally stable, is the main component of the raw materials, so the shell of the slow-release materials is very stable. The phenanthrene-contaminated groundwater interacts with the slow-release materials through cavities on the surface of the material. The shell can control the permeability of the packed layer. These properties ensure that the carbon and oxygen source are released slowly and persistently, thereby maximizing their useful life.

The longevity of a PRB is important for groundwater remediation [69,70]. The longevity is determined from the groundwater flow rates and the amount of reactive material consumed [71]. As shown in Fig. 5b, the material released oxygen for 350 days. While organic carbon was released continuously, its release from B was more stable than from A. When the groundwater velocity in column B was 0.48 m/d and the initial

porosity was approximately 24.1%, a total of 53.02 L of groundwater flowed through the column per year, resulting in an annual release of total organic carbon of 2.17 g. The total available carbon of column B was 26.65 g, so the PRB could last for at least 12.3 years, if the effect of armoring by secondary minerals in precipitation is ignored.

4. Conclusions

A novel PRB was tested for its ability to remediate PAH-contaminated groundwater *in situ*. This PRB was based on a microbe self-domestication mechanism, and combined adsorption and degradation processes to remove phenanthrene from groundwater. The PRB system naturally harbored genera of bacteria known for their ability to degrade phenanthrene and release organic carbon, which may maintain the microorganisms' capacity to degrade phenanthrene when the concentrations of phenanthrene were low. The release of organic carbon was more stable from material B than from material A. The new PRB material is a promising and cost-effective option as it is composed of inexpensive, readily-available materials and can be used in real applications.

Acknowledgements

We gratefully acknowledge the National Key Research and Development Program of China (2018YFD0800201), and the Environmental Protection Department of Jiangsu Province of China (Grant No. 2015009 and 2017001-1) for their financial support.

Appendix A. Supplementary data

General characteristics of raw materials used in the experiment (Table S1). The change of DO of phenanthrene with addition concentration at 0.9 mg/L every five days and repeated for 14 times in static experiments using A and B. Mean and standard error (n=3) (Figure S1).

References

[1] L. Ferreira, M. Cobas, T. Tavares, M.A. Sanroman, M. Pazos, Assessment of Arthrobacter viscosus as reactive medium for forming permeable reactive biobarrier applied to PAHs remediation, Environ. Sci. Pollut. Res. 20 (2013) 7348-7354.

[2] Y. Liang, M.F. Tse, L. Young, M.H. Wong, Distribution patterns of polycyclic aromatic hydrocarbons (PAHs) in the sediments and fish at Mai Po Marshes Nature Reserve, Hong Kong, Water Res. 41 (2007) 1303-1311.

[3] A. Bahr, A. Fischer, C. Vogt, P. Bombach, Evidence of polycyclic aromatic hydrocarbon biodegradation in a contaminated aquifer by combined application of in situ and laboratory microcosms using C-13-labelled target compounds, Water Res. 69 (2015) 100-109.

[4] R.J. Krupadam, M.S. Khan, S.R. Wate, Removal of probable human carcinogenic polycyclic aromatic hydrocarbons from contaminated water using molecularly imprinted polymer, Water Res. 44 (2010) 681-688.

[5] C. Gao, J. Wang, Research on Groundwater Organic Contamination Characteristics

in 69 Cities of China, Acta Geoscientia Sinica. 32 (2011) 581-591.

[6] C.F. Wu, H. Zhu, Y.M. Luo, J. Wang, Concentrations and potential health hazards of polycyclic aromatic hydrocarbon in shallow groundwater of a metal smelting area in Southeastern China, Sci. Total Environ. 569 (2016) 1561-1569.

[7] J.C. Lan, Y.C. Sun, S.Z. Xiao, D.X. Yuan, Polycyclic aromatic hydrocarbon contamination in a highly vulnerable underground river system in Chongqing, Southwest China, J. Geochem. Explor. 168 (2016) 65-71.

[8] X. Gong, Y. He, Y. Sun, Distribution and source of polycyclic aromatic hydrocarbons in groundwater in the upper region of Sihu Lake Basin from Jianghan Plain, Acta Scientiae Circumstantiae. 35 (2015) 789-796.

[9] Y.G. Zhang, M.Z. Liu, H.H. Chen, G.H. Hou, Source identification of polycyclic aromatic hydrocarbons in different ecological wetland components of the Qinkenpao Wetland in Northeast China, Ecotox. Environ. Safe. 102 (2014) 160-167.

[10] L. Kong, K. Kadokami, H.T. Duong, H.T.C. Chau, Screening of 1300 organic micro-pollutants in groundwater from Beijing and Tianjin, North China, Chemosphere. 165 (2016) 221-230.

[11] M.G. Waigi, F.X. Kang, C. Goikavi, W.T. Ling, Y.Z. Gao, Phenanthrene biodegradation by sphingomonads and its application in the contaminated soils and sediments: A review, Int. Biodeterior. Biodegrad. 104 (2015) 333-349.

[12] A.K. Haritash, C.P. Kaushik, Biodegradation aspects of Polycyclic Aromatic Hydrocarbons (PAHs): A review, J. Hazard. Mater. 169 (2009) 1-15.

[13] K. Lee, J.W. Park, I.S. Ahn, Effect of additional carbon source on naphthalene biodegradation by Pseudomonas putida G7, J. Hazard. Mater. 105 (2003) 157-167.

[14] C.-H. Yeh, C.-W. Lin, C.-H. Wu, A permeable reactive barrier for the bioremediation of BTEX-contaminated groundwater: Microbial community distribution and removal efficiencies, J. Hazard. Mater. 178 (2010) 74-80.

[15] G.X. Huang, F. Liu, Y.Z. Yang, W. Deng, S.P. Li, Y.Y. Huang, X.K. Kong, Removal of ammonium-nitrogen from groundwater using a fully passive permeable reactive barrier with oxygen-releasing compound and clinoptilolite, J. Environ. Manage. 154 (2015) 1-7.

[16] C.-W. Lin, C.-H. Wu, P.-Y. Guo, S.-H. Chang, Innovative encapsulated oxygen-releasing beads for bioremediation of BTEX at high concentration in groundwater, J. Environ. Manage. 204 (2017) 12-16.

[17] S.K. Mohanty, R. Valenca, A.W. Berger, I.K.M. Yu, X. Xiong, T.M. Saunders, D.C.W. Tsang, Plenty of room for carbon on the ground: Potential applications of biochar for stormwater treatment, Sci. Total Environ. 625 (2018) 1644-1658.

[18] K.J. Whaley-Martin, B.J. Mailloux, A. van Geen, B.C. Bostick, K.M. Ahmed, I. Choudhury, G.F. Slater, Human and livestock waste as a reduced carbon source contributing to the release of arsenic to shallow Bangladesh groundwater, Sci. Total Environ. 595 (2017) 63-71.

[19] A. Aloni, A. Brenner, Use of Cotton as a Carbon Source for Denitrification in Biofilters for Groundwater Remediation, Water. 9 (2017).

[20] J. Zhang, X. Jiang, C. Feng, H. Hao, Wheat straw, sawdust, and biodegradable plastics as potential carbon sources for synthetic nitrate-polluted groundwater column denitrification, Desalin. Water Treat. 77 (2017) 321-330.

[21] T. Li, W. Li, C. Feng, W. Hu, In-situ biological denitrification using pretreated maize stalks as carbon source for nitrate-contaminated groundwater remediation, Water Sci. Technol.-Water Supply. 17 (2017) 1-9.

[22] R. Wan, X. Zheng, Y. Chen, H. Wang, Using cassava distiller's dried grains as carbon and microbe sources to enhance denitrification of nitrate-contaminated groundwater, Appl. Microbiol. Biotechnol. 99 (2015) 2839-2847.

[23] X.M. Wang, J.L. Wang, Denitrification of nitrate-contaminated groundwater using biodegradable snack ware as carbon source under low-temperature condition, Int. J. Environ. Sci. Technol. 9 (2012) 113-118.

[24] Z. Jin, Y. Chen, N. Ogura, Using paper as the carbon source for groundwater nitrate removal, Yingyong Shengtai Xuebao. 15 (2004) 2359-2363.

[25] Y. Chen, Y. Cheng, Y. Jiang, Y. Yan, Z. Liu, Q. Tong, Z. Sun, Pump-and-treat method to remove nitrate from groundwater with liquor as the carbon source, Environ. Earth Sci. 76 (2017).

[26] L. Chu, J. Wang, Denitrification of groundwater using a biodegradable polymer as a carbon source: long-term performance and microbial diversity, RSC Adv. 7 (2017) 53454-53462.

[27] R. Zhang, Y. Zhang, F. Lv, H. Wang, S. Tu, Biological denitrification in simulated

groundwater using polybutylene succinate or polylactic acid-based composites as carbon source, Desalin. Water Treat. 57 (2016) 9925-9932.

[28] Q. He, C. Feng, Q. Hu, R. Li, N. Chen, Biological denitrification using rice washing drainage (RWD) as carbon source for removing nitrate from groundwater, Desalin. Water Treat. 57 (2016) 21990-21999.

[29] Y.S. Kim, K. Nakano, T.J. Lee, S. Kanchanatawee, M. Matsumura, On-site nitrate removal of groundwater by an immobilized psychrophilic denitrifier using soluble starch as a carbon source, J. Biosci. Bioeng. 93 (2002) 303-308.

[30] A. Basu, T.M. Johnson, Determination of hexavalent chromium reduction using Cr stable isotopes: isotopic fractionation factors for permeable reactive barrier materials, Environ. Sci. Technol. 46 (2012) 5353-5360.

[31] M. Ebert, R. Kober, A. Parbs, V. Plagentz, D. Schafer, A. Dahmke, Assessing degradation rates of chlorinated ethylenes in column experiments with commercial iron materials used in permeable reactive barriers, Environ. Sci. Technol. 40 (2006) 2004-2010.

[32] B. Flury, J. Frommer, U. Eggenberger, U. Mader, M. Nachtegaal, R. Kretzschmar, Assessment of Long-Term Performance and Chromate Reduction Mechanisms in a Field Scale Permeable Reactive Barrier, Environ. Sci. Technol. 43 (2009) 6786-6792.

[33] Y. Furukawa, J.-W. Kim, J. Watkins, R.T. Wilkin, Formation of ferrihydrite and associated iron corrosion products in permeable reactive barriers of zero-valent iron, Environ. Sci. Technol. 36 (2002) 5469-5475.

[34] K. Waybrant, C. Ptacek, D. Blowes, Treatment of mine drainage using permeable reactive barriers: column experiments, Environ. Sci. Technol. 36 (2002) 1349-1356.

[35] R. Köber, B. Daus, M. Ebert, J. Mattusch, E. Welter, A. Dahmke, Compost-based permeable reactive barriers for the source treatment of arsenic contaminations in aquifers: column studies and solid-phase investigations, Environ. Sci. Technol. 39 (2005) 7650-7655.

[36] F. Obiri-Nyarko, S.J. Grajales-Mesa, G. Malina, An overview of permeable reactive barriers for in situ sustainable groundwater remediation, Chemosphere. 111 (2014) 243-259.

[37] S. Gandhi, B.-T. Oh, J.L. Schnoor, P.J. Alvarez, Degradation of TCE, Cr (VI), sulfate, and nitrate mixtures by granular iron in flow-through columns under different microbial conditions, Water Res. 36 (2002) 1973-1982.

[38] R.T. Wilkin, C. Su, R.G. Ford, C.J. Paul, Chromium-removal processes during groundwater remediation by a zerovalent iron permeable reactive barrier, Environ. Sci. Technol. 39 (2005) 4599-4605.

[39] M. Cobas, L. Ferreira, M.A. Sanroman, M. Pazos, Assessment of sepiolite as a low-cost adsorbent for phenanthrene and pyrene removal: Kinetic and equilibrium studies, Ecol. Eng. 70 (2014) 287-294.

[40] D. Zhou, Y. Li, Y.B. Zhang, C. Zhang, X.F. Li, Z.L. Chen, J.Y. Huang, X. Li, G. Flores, M. Kamon, Column test-based optimization of the permeable reactive barrier (PRB) technique for remediating groundwater contaminated by landfill leachates, J.

Contam. Hydrol. 168 (2014) 1-16.

[41] S. Lee, A.H. Oren, C.H. Benson, K. Dovantzis, Organoclays as Variably Permeable Reactive Barrier Media to Manage NAPLs in Ground Water, J. Geotech. Geoenviron. Eng. 138 (2012) 115-127.

[42] R. Vignola, R. Bagatin, A.D.F. D'Auris, C. Flego, M. Nalli, D. Ghisletti, R. Millini, R. Sisto, Zeolites in a permeable reactive barrier (PRB): One year of field experience in a refinery groundwater-Part 1: The performances, Chem. Eng. J. 178 (2011) 204-209.

[43] R. Doherty, D.H. Phillips, K.L. McGeough, K.P. Walsh, R.M. Kalin, Development of modified flyash as a permeable reactive barrier medium for a former manufactured gas plant site, Northern Ireland, Environ. Geol. 50 (2006) 37-46.

[44] M. Cobas, L. Ferreira, T. Tavares, M.A. Sanroman, M. Pazos, Development of permeable reactive biobarrier for the removal of PAHs by Trichoderma longibrachiatum, Chemosphere. 91 (2013) 711-716.

[45] L. Ferreira, E. Rosales, M.A. Sanroman, M. Pazos, Preliminary testing and design of permeable bioreactive barrier for phenanthrene degradation by Pseudomonas stutzeri CECT 930 immobilized in hydrogel matrices, J. Chem. Technol. Biotechnol. 90 (2015) 500-506.

[46] O. Gibert, A.S. Ferguson, R.M. Kalin, R. Doherty, K.W. Dickson, K.L. McGeough, J. Robinson, R. Thomas, Performance of a sequential reactive barrier for Bioremediation of coal tar contaminated groundwater, Environ. Sci. Technol. 41 (2007) 6795-6801.

[47] S. Yuan, J. Chang, J. Yen, B.-V. Chang, Biodegradation of phenanthrene in river sediment, Chemosphere. 43 (2001) 273-278.

[48] K.J. Rockne, S.E. Strand, Biodegradation of bicyclic and polycyclic aromatic hydrocarbons in anaerobic enrichments, Environ. Sci. Technol. 32 (1998) 3962-3967.

[49] B.-P. Xin, C.-H. Wu, C.-H. Wu, C.-W. Lin, Bioaugmented remediation of high concentration BTEX-contaminated groundwater by permeable reactive barrier with immobilized bead, J. Hazard. Mater. 244 (2013) 765-772.

[50] Y. An, J. Li, N. Liu, Biological characteristics of the nitrobenzene-degrading strain NB1 during bioaugmentation of nitrobenzene-contaminated groundwater, Environ. Earth Sci. 75 (2016).

[51] E.D. Samuelsen, N. Badawi, O. Nybroe, S.R. Sorensen, J. Aamand, Adhesion to sand and ability to mineralise low pesticide concentrations are required for efficient bioaugmentation of flow-through sand filters, Appl. Microbiol. Biotechnol. 101 (2017) 411-421.

[52] M.G. Gomez, C.M. Anderson, C.M.R. Graddy, J.T. DeJong, D.C. Nelson, T.R. Ginn, Large-Scale Comparison of Bioaugmentation and Biostimulation Approaches for Biocementation of Sands, J. Geotech. Geoenviron. Eng. 143 (2017).

[53] J.C. Araujo, F.C. Téran, R.A. Oliveira, E.A. Nour, M.A. Montenegro, J.R. Campos, R.F. Vazoller, Comparison of hexamethyldisilazane and critical point drying treatments for SEM analysis of anaerobic biofilms and granular sludge, J. Electron Microsc. 52 (2003) 429-433.

[54] T. Van Nooten, D. Springael, L. Bastiaens, Positive impact of microorganisms on the performance of laboratory-scale permeable reactive iron barriers, Environ. Sci. Technol. 42 (2008) 1680-1686.

[55] J.G. Caporaso, C.L. Lauber, W.A. Walters, D. Berg-Lyons, J. Huntley, N. Fierer, S.M. Owens, J. Betley, L. Fraser, M. Bauer, Ultra-high-throughput microbial community analysis on the Illumina HiSeq and MiSeq platforms, ISME J. 6 (2012) 1621-1624.

[56] J.G. Caporaso, C.L. Lauber, W.A. Walters, D. Berg-Lyons, C.A. Lozupone, P.J. Turnbaugh, N. Fierer, R. Knight, Global patterns of 16S rRNA diversity at a depth of millions of sequences per sample, Proc. Natl. Acad. Sci. U. S. A. 108 (2011) 4516-4522.

[57] Q. Wang, G.M. Garrity, J.M. Tiedje, J.R. Cole, Naive Bayesian classifier for rapid assignment of rRNA sequences into the new bacterial taxonomy, Appl. Environ. Microbiol. 73 (2007) 5261-5267.

[58] Y. Yao, G.H. Huang, C.J. An, G.H. Cheng, J. Wei, Effects of freeze-thawing cycles on desorption behaviors of PAH-contaminated soil in the presence of a biosurfactant: a case study in western Canada, Environ. Sci.-Process Impacts. 19 (2017) 874-882.

[59] J. Liu, L.L. He, F.Q. Dong, K.A. Hudson-Edwards, The role of nano-sized manganese coatings on bone char in removing arsenic(V) from solution: Implications for permeable reactive barrier technologies, Chemosphere. 153 (2016) 146-154.

[60] Z.M. Chen, H.Y. Wang, X.W. Liu, X.L. Zhao, D.J. Lu, J.M. Zhou, C.Z. Li, Changes in soil microbial community and organic carbon fractions under short-term straw return

in a rice-wheat cropping system, Soil Tillage Res. 165 (2017) 121-127.

[61] J.M. Holding, C.M. Duarte, A. Delgado-Huertas, K. Soetaert, J.E. Vonk, S. Agusti, P. Wassmann, J.J. Middelburg, Autochthonous and allochthonous contributions of organic carbon to microbial food webs in Svalbard fjords, Limnol. Oceanogr. 62 (2017) 1307-1323.

[62] M. Crampon, A. Cebron, F. Portet-Koltalo, S. Uroz, F. Le Derf, J. Bodilis, Low effect of phenanthrene bioaccessibility on its biodegradation in diffusely contaminated soil, Environ. Pollut. 225 (2017) 663-673.

[63] K.A. Hiller, K.H. Foreman, D. Weisman, J.L. Bowen, Permeable Reactive Barriers Designed To Mitigate Eutrophication Alter Bacterial Community Composition and Aquifer Redox Conditions, Appl. Environ. Microbiol. 81 (2015) 7114-7124.

[64] Y.F. Ma, L. Wang, Z.Z. Shao, Pseudomonas, the dominant polycyclic aromatic hydrocarbon-degrading bacteria isolated from Antarctic soils and the role of large plasmids in horizontal gene transfer, Environ. Microbiol. 8 (2006) 455-465.

[65] O. Kweon, S.J. Kim, J. Blom, S.K. Kim, B.S. Kim, D.H. Baek, S.I. Park, J.B. Sutherland, C.E. Cerniglia, Comparative functional pan-genome analyses to build connections between genomic dynamics and phenotypic evolution in polycyclic aromatic hydrocarbon metabolism in the genus Mycobacterium, BMC Evol. Biol. 15 (2015) 23.

[66] G.F. Ma, F.T. Ran, E.K. Feng, Z. Zhang, Z.Q. Lei, Preparation and properties of an organic-inorganic composite superabsorbent based on attapulgite, J. Compos Mater.

50 (2016) 1865-1874.

[67] C.K.O. da Silva-Rackov, W.A. Lawal, P.A. Nfodzo, M. Vianna, C.A.O. do Nascimento, H. Choi, Degradation of PFOA by hydrogen peroxide and persulfate activated by iron-modified diatomite, Appl. Catal. B-Environ. 192 (2016) 253-259.

[68] D. Tavakoli, A. Tarighat, Molecular dynamics study on the mechanical properties of Portland cement clinker phases, Comput. Mater. Sci. 119 (2016) 65-73.

[69] L. Carniato, G. Schoups, P. Seuntjens, T. Van Nooten, Q. Simons, L. Bastiaens, Predicting longevity of iron permeable reactive barriers using multiple iron deactivation models, J. Contam. Hydrol. 142 (2012) 93-108.

[70] J. Klausen, P.J. Vikesland, T. Kohn, D.R. Burris, W.P. Ball, A.L. Roberts, Longevity of granular iron in groundwater treatment processes: Solution composition effects on reduction of organohalides and nitroaromatic compounds, Environ. Sci. Technol. 37 (2003) 1208-1218.

[71] U. Pathirage, B. Indraratna, Assessment of optimum width and longevity of a permeable reactive barrier installed in an acid sulfate soil terrain, Can. Geotech. J. 52 (2015) 999-1004.

Table Captions

Table 1. The desorption concentrations of phenanthrene in solid samples from the 4 sampling ports of columns A and B after 450 days.

Column	SP1 (mg/L)	SP2 (mg/L)	SP3 (mg/L)	SP4 (mg/L)
A	0.03	-	-	-
B	0.02	-	-	-

Figure Captions

Fig. 1. The configuration of a treatment column.

Fig. 2. Nitrogen adsorption-desorption isotherms of materials A and B and BJH desorption average pore diameter distribution.

Fig. 3. The adsorption kinetics of phenanthrene on materials A and B (with an initial pH of 7.0 and an initial phenanthrene concentration of 0.9 mg/L).

Fig. 4. The phenanthrene removal efficiency of materials A and B. Phenanthrene was added repeatedly at a concentration of 0.9 mg/L every 5 days. Mean and standard error (n=3).

Fig. 5. (a) Changes in the pH value from sampling ports SP1, SP2, SP3, and SP4 after 200 days. Comparisons of the (b) dissolved oxygen concentration and (c) total organic carbon as a function of time in the influent and the effluent groundwater in columns A and B over the 450-day period. The peristaltic pump flow rate was 126.89 μL/min.

Fig. 6. ESEM images show how the surface morphology of the materials changed after the 200-day column experiments. A) Material A before the experiment; B) Material B before the experiment; C) Material A after 200 days in the flow-through column; D) Material B after 200 days in the flow-through column.

Fig. 7. Principal coordinates analysis (PCoA) of bacterial community structures using (a) weighted UniFrac distances, (b) the total numbers of eubacterial 16S rDNA genes and (c) the relative abundance at genus level of phenanthrene degraders from the initial, SP1, SP2, SP3, and SP4 materials of every column.

Fig. 1

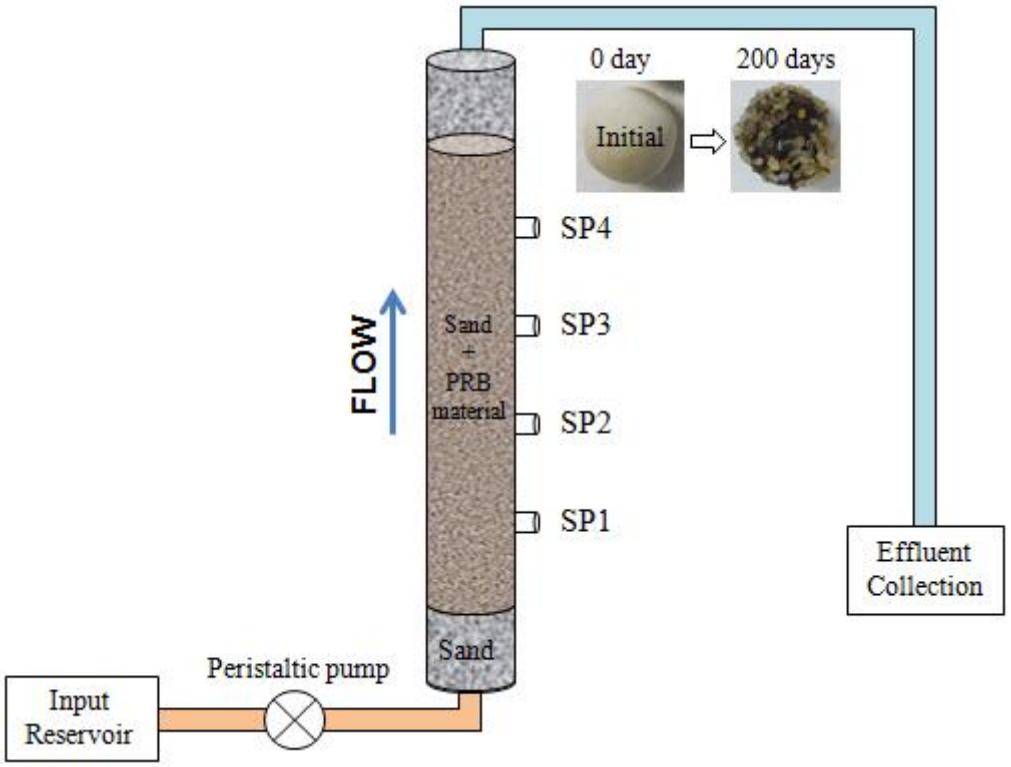
0 day
200 days
Initial
SP4
SP3
SP2
SP1
FLOW
Sand
+
PRB
material
Sand
Effluent
Collection
Peristaltic pump
Input
Reservoir

Fig. 2

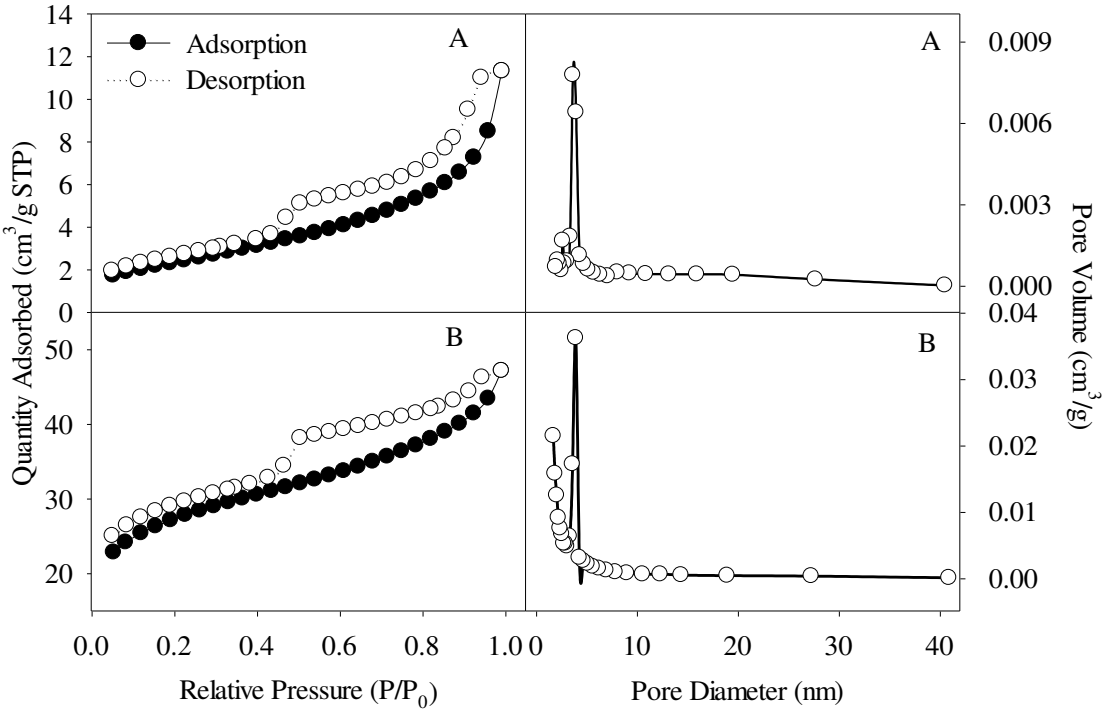
Adsorption
Desorption
A
B
Quantity Adsorbed (cm3/g STP)
Relative Pressure (P/P0)
Pore Diameter (nm)
Pore Volume (cm3/g)

Fig. 3

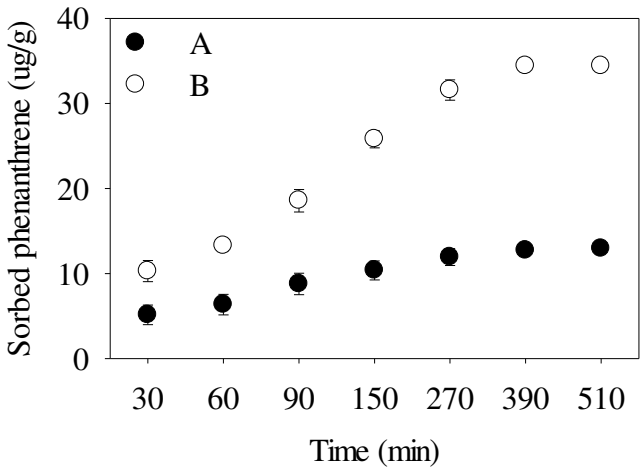
Sorbed phenanthrene (ug/g)
40
30
20
10
0
A
B
30
60
90
150
270
390
510
Time (min)

Fig. 4

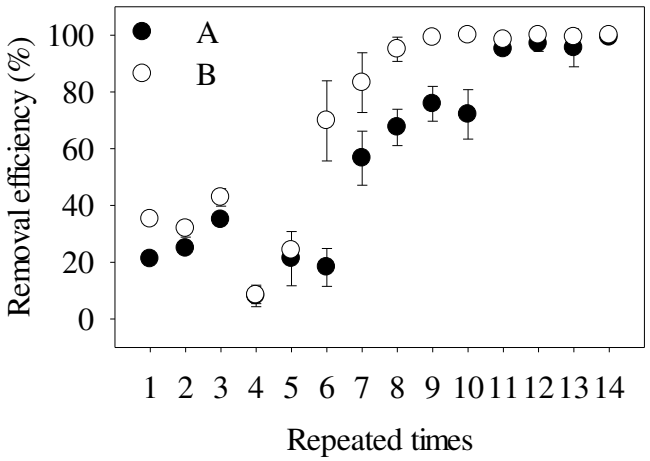
Removal efficiency (%)
100
80
60
40
20
0
A
B
1
2
3
4
5
6
7
8
9
10
11
12
13
14
Repeated times

Fig. 5

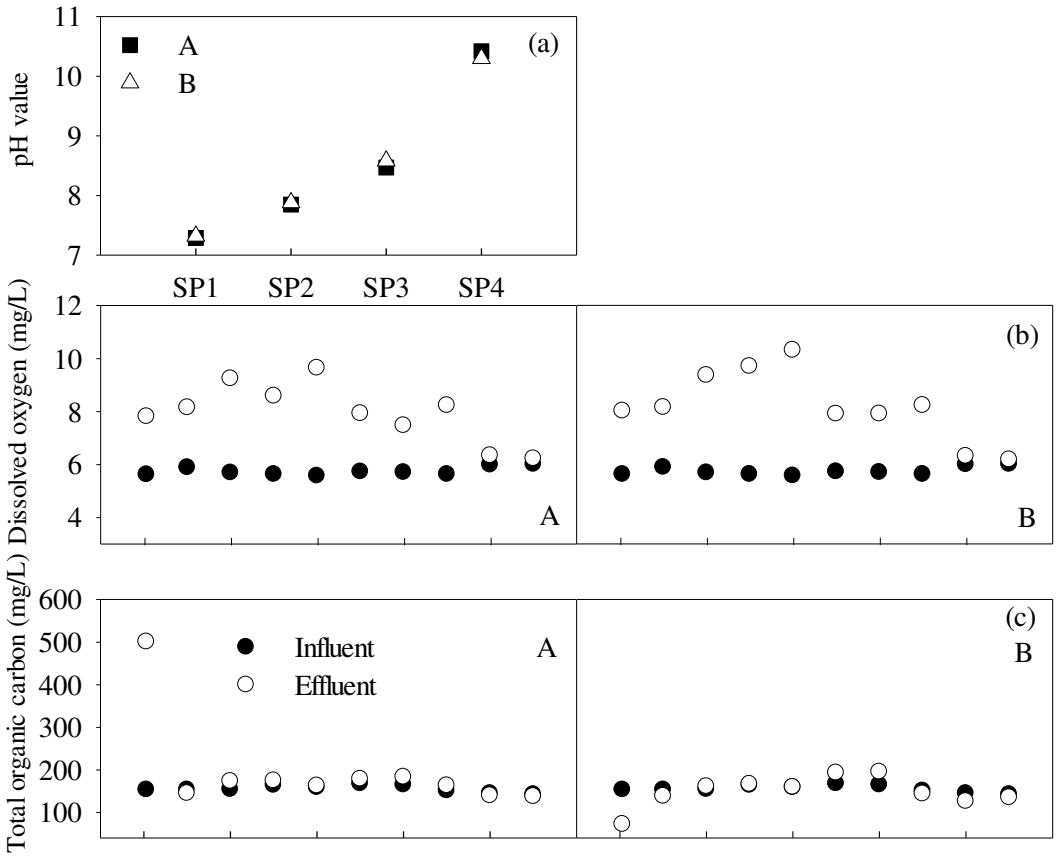
pH value
11
10
9
8
7
A
B
(a)
SP1
SP2
SP3
SP4
Dissolved oxygen (mg/L)
12
10
8
6
4
(b)
A
B
Total organic carbon (mg/L)
600
500
400
300
200
100
Influent
Effluent
(c)
A
B

Fig. 6

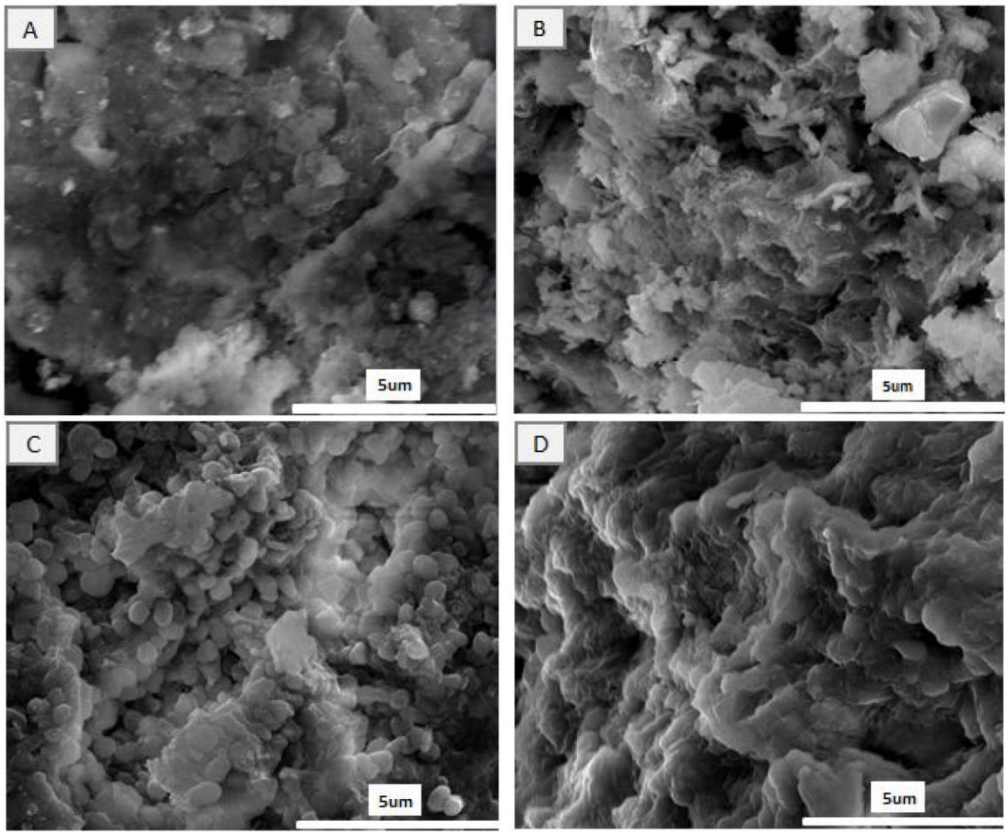

Fig. 7

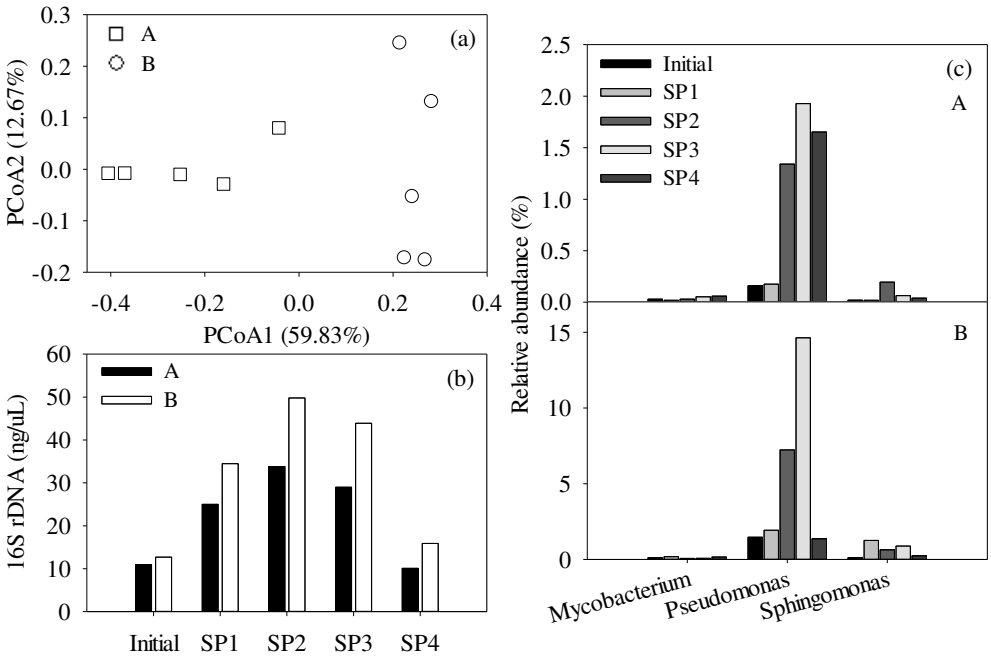
(a)
A
B
PCoA2 (12.67%)
PCoA1 (59.83%)
(b)
16S rDNA (ng/uL)
Initial
SP1
SP2
SP3
SP4
(c)
Relative abundance (%)
Mycobacterium
Pseudomonas
Sphingomonas